Effect of Morphology and Non-Bounded Interface on Dielectric Properties of Plasma Sprayed Batio$_3$ Coating

A. H. Paksereshta,*, M. R. Rahimipoura, M. R. Vaezib, M. Salehic

[a] *Department of Ceramics, Materials and Energy Research Center, karaj, Iran.*
[b] *Department of Nanotechnology and Advanced Materials, Materials and Energy Research Center, karaj, Iran.*
[c] *Department of Materials Engineering, Isfahan University of Technology, Isfahan, Iran.*

ARTICLE INFO

Article history:

Received 28 March 2014
Accepted 24 Sep. 2014
Available online 01 Dec. 2014

Keywords:

Plasma spray
$BaTiO_3$
Dielectric constant
Amorphous phase
Non-bounded interface

ABSTRACT

In this research, $BaTiO_3$ thick deposit has been successfully sprayed by air plasma spray. Microstructure and dielectric properties of the thick films were investigated by scanning electron microscopy (SEM) and LCR meter, respectively. XRD measurement was also carried out on the plasma sprayed $BaTiO_3$. The results illustrate differences in the crystal structure between the plasma sprayed coatings and the feedstock powders. The as-deposited films were mainly crystalline with a small amount of an amorphous second phase. The ratio of crystalline–to-amorphous phases was found to be critically dependent on the degree of melting of feed stock powders. The as-deposited $BaTiO_3$ films had maximum dielectric constant as high as 85 at room temperature. Upon annealing in air at 1050℃, the dielectric constant increased to165. The increase in dielectric constant was attributed to the crystallization of the amorphous phase. The dielectric constant of plasma sprayed $BaTiO_3$ thick films was lower than that of sintering ceramic. Reduction in dielectric properties of deposited films was related to splats interface and lamellar structure of plasma sprayed coatings.

1. Introduction

Barium titanate is a ferroelectric ceramic material with a perovskite structure. It has four isomorphs, namely rhombohedral, orthorhombic, tetragonal and cubic. There is also a hexagonal form which is stable above ~1430°C. The tetragonal form of $BaTiO_3$ is stable at room temperature, whereas the polar form (cubic) is stable above ~130°C. By decreasing the temperature below curie temperature (130°C), spontaneous polarization happens in $BaTiO_3$ and phase transition occurs in the crystal. Therefore, cubic form structure transforms to tetragonal. It should be noticed that all forms of $BaTiO_3$ have relatively high dielectric constants [1-3].

Barium titanate is very promising for a wide range of applications like multilayer ceramic capacitors (MLCCs), piezoelectric and infrared sensors, and electro-optics devices because of high dielectric constant, low dielectric loss, high chemical and mechanical stability, low temperature coefficient of dielectric constant, the composition-dependent curie temperature, and easy preparation methods [4-5]. In addition, it is utilized in positive temperature coefficient resistors (PTCR) such as thermistors, electroluminescent panels, and

Corresponding author:
E-mail address: amirh_pak@yahoo.com (Amirhossein. Pakseresht).

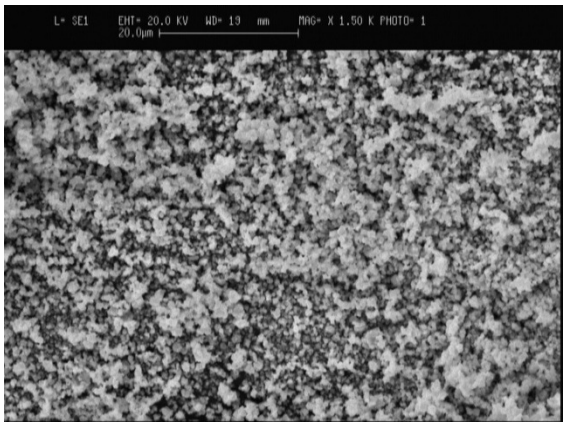

Fig. 1. Morphology of feedstock powders

pyroelectric elements [4-5]. In general, barium titanate has different behavior in the form of monocrystal, bulk material, and thin film [6].

So many methods such as rf-magnetron sputtering, reactive evaporation, laser deposition, chemical solution deposition, sol gel, spin coating, dip coating, screen printing, thermal spray, and metallic organic chemical vapor deposition have been used to prepare $BaTiO_3$ coating. Generally, when the film thickness increases, the difficulty in creating the thick deposit is well understood [7-9].

Among the preparation methods, plasma spray can create layers with "bulk –like" thickness, but adhering on a metallic substrate with various shapes. Plasma spray is usually used to make anti wear, corrosion, erosion, and thermal barrier coating [6]. Indeed, with the improvement of technology, the need to use plasma spray in all industries (such as magnetic, electric and biomaterial) is more urgently felt [10]. Nowadays, thermal spray shows an array of unique attributes and advantages in thick-film electronics and sensor fabrication. It is cost-effective, efficiently processable in virtually any environment and can be applied on a wide range of substrates [6, 10]. However, up to now, among dielectric materials barium titanate has seldom been sprayed and understanding of its properties in the form of coating necessitates further research. In this process, the plasma sprayed $BaTiO_3$ properties were affected by micro crack, voids formation, splat morphology, and splat interfaces within the coating [10-14].

In this investigation, barium titanate powder has been sprayed onto the stainless steel substrate by atmospheric plasma spraying. Microstructure and hardness were examined for producing thick films. Furthermore, electrical properties such as dielectric constant have been evaluated in the application of electronic instruments and the effect of non-bounded interface in the sprayed coating has been surveyed.

2. Experimental

2. 1. Materials

The disk-like stainless steel samples with 20 mm diameter and 5 mm thickness were used as the substrate. The samples were grit blasted with alumina particles to roughen the surface for improvement in the adhesion strength. Barium titanate (Alfa Company code No. 12348) was used as feedstock powder, and feed powder sizes were -325 mesh (< 44µm) Fig. 1 shows the morphology feedstock powders. Because feedstock powders didn't have enough flowbility, plasma spraying of the powders was impossible. In order to remove this obstacle, they should be granulated properly. In order to granulate the powders, at first a specific amount of hydro soluble polyvinyl alcohol (PVA) (Junsel Chemical Co. Ltd., Japan) was added as a binder to distilled water and stirred for 30 min at 50°C until PVA was completely solute. Then, the $BaTiO_3$ powder was gradually added and the suspension was stirred again for an additional 45 min. After that, the obtained slurry was heated in the oven for 8 hours at 100 °C until the water was completely removed. Then, the dried materials were crushed and the obtained powders were sieved. The size ranges for the sieved powder were nominally –100 µm with a mean of 60 µm. The morphology of the granule particles is shown in Fig. 2. After granulation, the granules could be fed into the APS system.

2. 2. Air plasma spraying

Plasma spraying was performed with a Plasma Technique AG; Metco 3MB gun in air. Argon gas was the primary plasma gas and hydrogen was added as the secondary gas. The powders were sprayed based on the standard parameters suggested by the Sulzer-Metco for titanate base

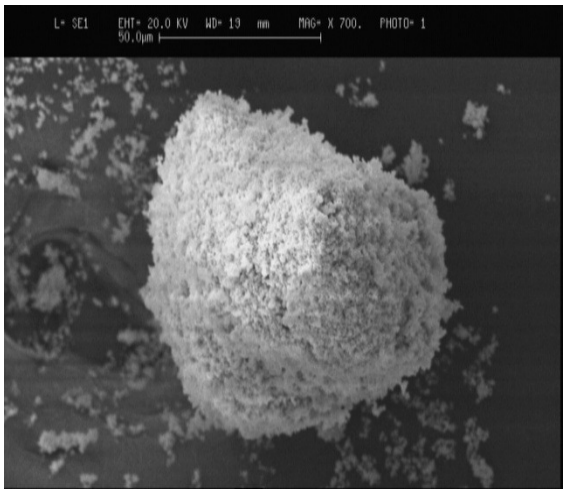

Fig. 2. Morphology of granulated powders

materials. The spraying parameters are shown in Table 1. In order to raise the coating adhesion, the substrates were degreased and cleaned with acetone. The sprayed coating, which was formed directly on the substrate, was cooled by air blowing. Spray distance was about 140 mm. In order to fix the samples and spraying distance, the fixture was used.

2. 3. Microstructure analysis

For microscopic observation and for microhardness measurements, polished cross-sections as well as in-plane sections of the coatings were prepared. Conventional microhardness of the coatings was measured by an optical microscope equipped and Vickers indenter using 50 gf load applied over 15s (MVK-H21). The mean value of microhardness was calculated as an average from 10 indentations, which were aligned to create microhardness profiles from the coating surface to the substrate.

Microstructural investigation of the plasma sprayed coatings was carried out on the top surface and the cross-section using scanning electron microscopy (S360 Cambridge 1990). X-ray diffraction (XRD: Philips Mode PW 3710) analysis was performed using Cu-Kα at 40 kV and 30 mA. The analyzed range of the diffraction angle (2θ) was between 10° and 70°, with a step width of 0.02°.

2. 4. Dielectric properties

For the electrical properties, the top surface of coating was contacted by sputtered gold electrodes and the substrate was used as bottom electrode. Dielectric properties (dielectric constant and dielectric loss) were measured by the LCR - meter model (Precision LCR Meter 8110G) at 1 KHz and with 1 V AC perpendicular to the coating surface. All measurements were performed at the same humidity condition [15]. Relative permittivity of materials is related to the materials dimensions and was calculated from measured capacities C_P, according to the equation 1.

$$C_P = \varepsilon_0 \times \varepsilon r \times A/t \quad [1]$$

Where $\varepsilon_0 = 8.854 \times 10^{-12}$ F m^{-1}; A/t [m] is defined as the ratio between the area of electrode and the thickness of the layer. The same condition and equipment was applied for the loss tangent measurement.

Table 1. Parameters of air plasma spraying

Parameter	Value
Current(A)	400
Voltage(V)	60
Primary gas, Ar (SCFH)	80
Secondary gas , H_2 (SCFH)	10
Powder feed rate (g/min)	20
Spray distance (mm)	140

3. Result and discussion

3. 1. Microstructure study

Fig. 3 shows the top surface of $BaTiO_3$ coatings, and indicates the presence of unmelted particles (U), micro-cracks (C), and melted splats (S). It was observed that the $BaTiO_3$ coatings presented a bimodal structure, which means the presence of two phases which were described as melted and unmelted parts. The unmelted part of the coating is surrounded by fully molten particles that act as a binder, thereby maintaining coating integrity. The top surface of the as-deposited film is rough and contains voids and micro cracks, typical for plasma-spray deposits. The microcracks were formed because of the release of residual stress resulted from the spray process. Also, micron-sized voids were formed in the coating. The splat was formed by the impact of droplets on the substrate and rapid solidification of them. The thin splat layering caused by deformation of the powder particles on impact is typical of the APS process. The morphology of individual

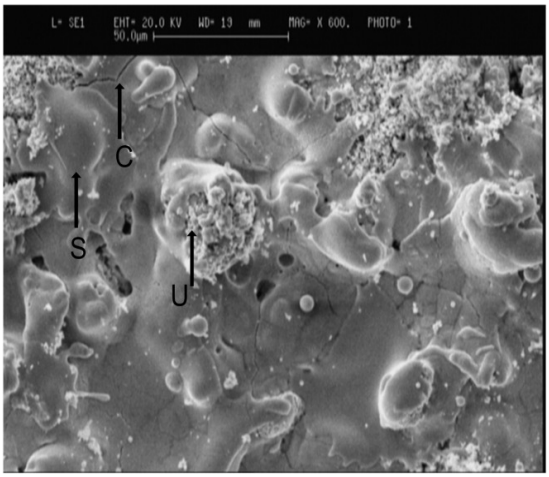

Fig. 3. Top view of APS deposited BT. Splat (S), Cracking (C), Unmelted zone (U)

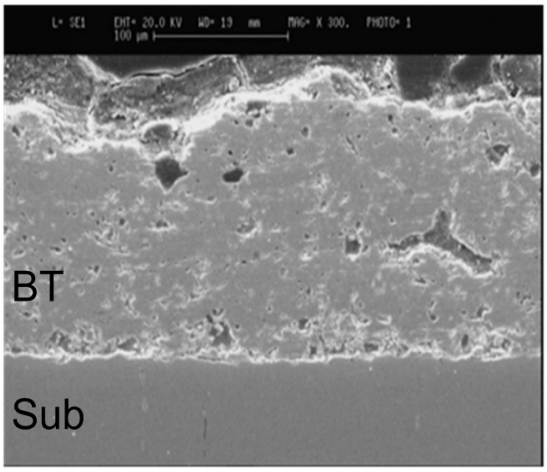

Fig. 4. The polished cross-section morphology of as-sprayed BT

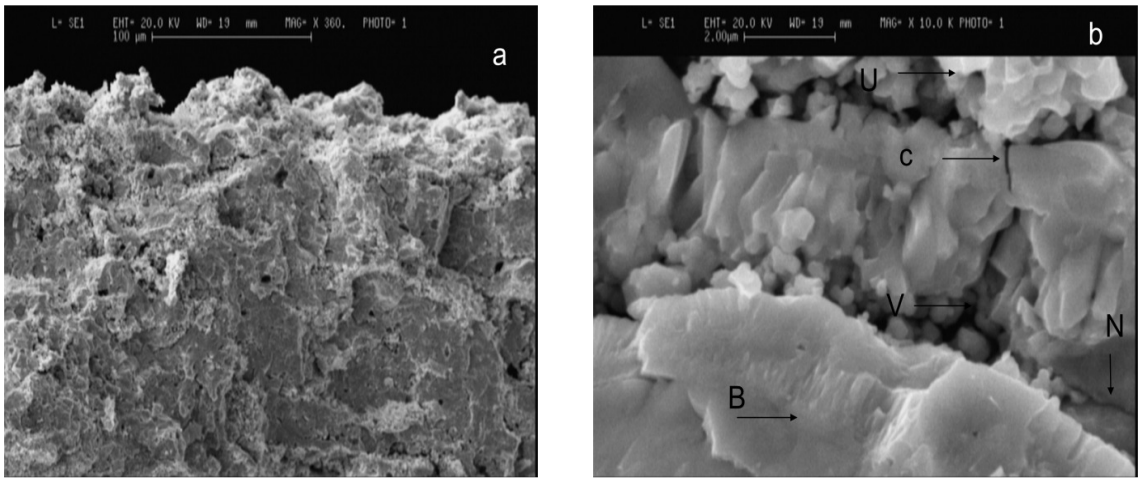

Fig. 5. The fractured cross-section morphology of as-sprayed BT (a) Overview (b) More Magnification

splat can effect on electrical and mechanical properties of the coating. Coating with splash splats has higher porosity than coating with disk splats and it can influence the properties of coating. Based on Fig 3 in this process, like the usual plasma spray process, the splats have splash morphology.

Fig. 4 shows the polished cross-section morphology of the as-sprayed $BaTiO_3$ coating, which is relatively dense with some common defects of the plasma spray process. Melted/ non-melted area porosities and voids can be seen in this image. Fig. 5 illustrates the fractured cross-section morphology of the fractured $BaTiO_3$ film. As shown in Fig. 5, the observed cross-sectional microstructure is typical of $BaTiO_3$ coatings with dense area (melted area), micro-cracks, spheroidal pore, splats and unmelted zone (unmelted or partially melted particles). It showed characteristic lamellar microstructure of built up of many individual splats, a thin layer of voids resulting from poor inter splat contact separating them. The lamellar structure is characterized by the interfaces between lamellar which are presented as inter-lamellar. In the melted area, the coating consisted of typical lamellar structures which indicates that the coating was deposited by molten spray particles. The columnar grain structure in a direction perpendicular to the lamellar plane can also be clearly observed in individual splats. Although local bonding is obvious at some lamellar interfaces in the $BaTiO_3$ deposit, as indicated by arrow B, most splat interfaces have a non-bonded interface, as indicated by arrow

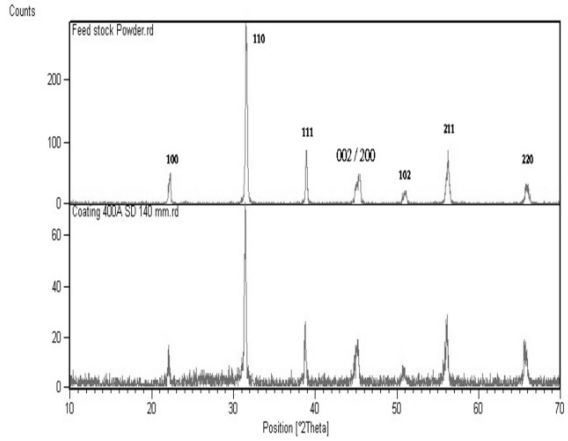

Fig. 6. The XRD pattern of the powders and coating

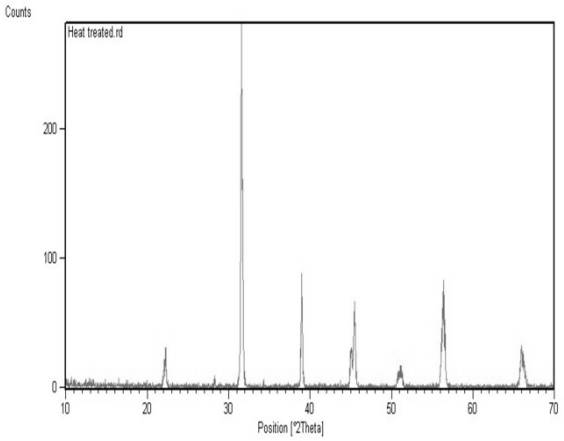

Fig. 7. The XRD pattern of the coating after heat treatment

Table 2. Dielectric constant and loss tangent of as-sprayed and annealed $BaTiO_3$ coating

Sample	Dielectric constant	Loss tangent
As-deposited Coating	85	0.09
Heat treated Coating	165	0.08

N. They are also clearly observed beside the cracks (marked by C) perpendicular to the lamellar structure and between the two splats. It is not possible to obtain quantitatively a reliable fraction of the bonded interfaces, because it is not clear how the fracture influences the debonding. Meanwhile, it was found that some unmelted feedstock particles were distributed between the splats. These particles saved the initial microstructure of feedstock (marked by U). Some voids between splats were also observed (marked by V).

The result of microhardness test shows the value of the coating fluctuated from 500 to 540 $HV_{0.5}$. So, in some part of the film the hardness value of the BT coating decreases obviously to 350 HV and it is due to the existence of pore and crack that has a lower hardness.

3. 2. Structure studies

Fig. 6 shows the XRD pattern of feedstock $BaTiO_3$ powder and crystallinity of the plasma spray deposited $BaTiO_3$ film. It shows two distinct (002) and (200) diffraction peaks, indicating that the powder and the film have tetragonal phase (PDF Card No.01-074-2491). According to the pattern, except for the polycrystalline tetragonal $BaTiO_3$, no other crystalline phases are observed in the film. In addition to $BaTiO_3$ crystalline phase peaks, there is a high diffuse background in the range of 24-30°, which is attributed to an amorphous phase. The presence of an amorphous phase in the as-sprayed $BaTiO_3$ coating is expected, since some parts of plasma-spray-deposited film experience rapid quenching during the spray process. Crystalline phase also remained due to the existence of partially molten droplets and other non-rapid quenching splats.

To determine the effect of heat treatment, the samples were heated at 1050°C for 3 h. Fig.7 shows the XRD pattern of $BaTiO_3$ film after heat treatment. It was demonstrated that the amorphous phase changed into the crystalline phase by heat treatment.

3. 3. Dielectric Properties

Dielectric properties were measured on the as-deposited and heat treated samples. The thickness of the as-deposited film was 200± 30 μm. Dielectric constants for the $BaTiO_3$ deposited by plasma systems are presented in table 2.

As a result of heat treatment, the amorphous phase in the as–sprayed coating was crystallized to $BaTiO_3$; therefore, the dielectric constant of $BaTiO_3$ film increases. It indicates the amount of amorphous phases reduced in deposited films. From the XRD results of the plasma deposited layers, it can be inferred that the higher dielectric constants are achieved by

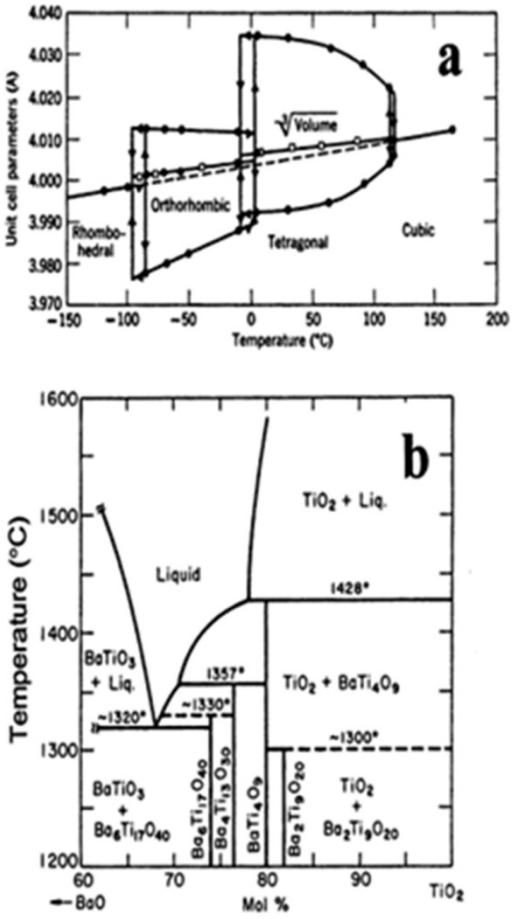

Fig. 8. (a) The relationship for $BaTiO_3$ between unit cell parameters and temperature. (b) BaO–TiO_2 phase diagram (showing the eutectic to form the $BaTiO_3$ phase from the liquid) [11]

an increase in the proportion of crystalline phase and a decrease in voids, non-bounded interface and cracking within the deposit. Crystalline $BaTiO_3$ has a higher dielectric constant than amorphous $BaTiO_3$, whereas the defects of the deposit introduce air gaps in the structure and reduce dielectric property [10-11].

A direct comparison can therefore be made between crystallinity and dielectric properties. It is well known that the dielectric constants of a polycrystalline material enhance with an increase in grain boundary surface area [10-11]. Hence, the increase in the crystallinity of the film gives a higher dielectric value. However, the amount of the crystalline phase is not the only reason governing the dielectric constant. The relation between crystallinity and deposition parameters may be clarified by understanding the temperature history of the particles as they are fed through the torch and are accelerated onto the substrate. According to the diagram demonstrated in Fig. 8(a), $BaTiO_3$ changes from cubic to tetragonal phase on cooling below 130°C. However, because of the eutectic to the right of stoichiometric $BaTiO_3$, as seen in the phase diagram in Fig. 8(b), [11] adequately rapid cooling of this phase might prevent the transition to the crystalline state, and forming an amorphous phase, instead. Typical cooling rates for particles impinging on a cold substrate can reach values of up to 10^7 Ks^{-1} [10-11]. Thus, the amorphous structure of the $BaTiO_3$ coating is to be expected and it can decrease dielectric constant; to remove this problem heat treatment of deposit can enhance dielectric properties.

4. Conclusion

$BaTiO_3$ has been successfully sprayed by air plasma spray as dielectric layers. The degree of crystallinity and morphology of the coating are two important factors that influence the dielectric property of the plasma sprayed coating. Coatings with more crystalline phase show higher dielectric constant. Voids, micro cracks, and interface splats reduce dielectric constant and should be controlled in the process. The as-deposited $BaTiO_3$ films had dielectric constant as high as 85 in 200 μm thick layers. After annealing in air, the dielectric constant increased to 165.

References

1. U. M. Pasha, H. Zheng, O. Thakur, A. Feteira, D. C. Sinclair, and I. M. Reaney, "In situ Raman spectroscopy of A-site doped barium titanate", *Applied Physics Letters*, Vol. 91, 2007, pp. 62-65.
2. Y. Iqbal, A. Jamal, R. Ullah, M. N. Khan, and R. Ubic, "Effect of fluxing additive on sintering temperature , microstructure and properties of BaTiO3",Buellton Material Science, Vol. 35, no. 3, 2012, pp. 387–394.
3. A. J. Bell, "Ferroelectrics: The role of ceramic science and engineering ", Journal of European Ceramic, Vol. 28, 2008, pp. 1307-1317.
4. A. Abdel Aal, M. Rashad, G. Amin, "Dielectric

thin film from barium titanate nanopowders", Journal of Physics, vol. 1, 2007, pp. 1–6.
5. A. Jamal, M. Naeem, Y. Iqbal, "Characterization of barium titanate prepared via mixed oxide sintering route", Journal of Pakistan Material Society, Vol. 2, no. 2, 2008, pp. 91–95.
6. P. Ctibor, H. Ageorges, J. Sedlacek, and R. Ctvrtlik, "Structure and properties of plasma sprayed BaTiO3 coatings", Ceramics International, Vol. 36, no. 7, 2010, pp. 2155–2162.
7. G. Gomez-Yanez, C. Benitez, H. Balmori-Ramirez, "Mechanical activation of the synthesis reaction of BaTiO3 from a mixture of BaCO3 and TiO2 powders", Ceramics International, Vol. 26, 2000, pp. 271–277.
8. M. Prudenziati, R. dell'Acqua in: M. Prudenziati (Ed.), Thick film resistors, Elsevier Science, Amsterdam, 1994.
9. B. D. Stojanovic, C. R. Foschini, V. B. Pavlovic, and V. M. Pavlovic, "Barium titanate screen-printed thick films" , Ceramics International , Vol. 28, 2002, pp. 293–298.
10. S. Sampath, "Thermal Spray Applications in Electronics and Sensors: Past, Present, and Future", Journal of thermal spray technology, Vol. 19, 2010, pp. 921–949.
11. A. H. Dent, A. Patel, J. Gutleber, E. Tormey, S. Sampath, H. Herman, "High velocity oxy-fuel and plasma deposition of BaTiO3 and (Ba,Sr)TiO3", Materials Science and Engineering B , Vol. 87, 2001, pp.23–30.
12. C. Li, G. Yang, and C. Li, "Development of particle interface bonding in thermal spray coatings: A Review", Journal of thermal spray technology, Vol. 22, 2013, pp. 192–206.
13. X. Ning, C. Li, G. Yang, "Modification of microstructure and electrical conductivity of plasma-sprayed YSZ deposit through post-densification process" , Materials Science and Engineering A, Vol. 428, 2006, pp. 98–105.
14. Y. Xing, C. Li, G. Yang, "Influence of through-lamella grain growth on ionic conductivity of plasma-sprayed yttria-stabilized zirconia as an electrolyte in solid oxide fuel cells", Journal of Power Sources ,Vol. 176, 2008, pp. 31–38.
15. P. Ctibor, J. Sedlacek, K. Neufuss, P. Chraska, "Dielectric relaxation in calcium titanate-containing ceramics prepared by plasma spraying", Ceramics International, vol. 29, 2003, pp. 955–960.